ChemComm

COMMUNICATION

View Article Online
View Journal | View Issue

Cite this: *Chem. Commun.*, 2017, 53, 4266

Received 21st February 2017,
Accepted 23rd March 2017

DOI: 10.1039/c7cc01382e

rsc.li/chemcomm

A family of 'windmill'-like $\{Cu_6Ln_{12}\}$ complexes exhibiting single-molecule magnetism behavior and large magnetic entropy changes†

Dimitris I. Alexandropoulos,[a] Katye M. Poole,[b] Luis Cunha-Silva,[c] Javeed Ahmad Sheikh,[d] Wolfgang Wernsdorfer,[efg] George Christou[b] and Theocharis C. Stamatatos*[a]

A family of nanosized $\{Cu_6Ln_{12}\}$ clusters with a 'windmill'-like topology was prepared from the employment of 2,6-diacetylpyridine dioxime, in conjunction with bridging N_3^-, in 3d/4f-metal chemistry; the octadecanuclear compounds exhibit single-molecule magnetism behavior and large magnetic entropy changes, depending on the 4f-metal ion present.

The search for polynuclear metal complexes (or clusters) with new structural motifs and interesting properties, such as magnetic, optical and catalytic, continues to attract the interest of the academic community for a number of reasons.[1] These include, but are not limited to: (i) the synthesis of nanoscale molecular materials with large nuclearities and unique structures,[2] (ii) the isolation of high-spin molecules and single-molecule magnets (SMMs) with large spin ground state values and energy barriers (U) for the magnetization reversal,[3] and (iii) the synthesis of molecular magnetic refrigerants with enhanced magnetocaloric properties as alternatives to low-temperature cooling applications.[4] SMMs are molecular species that show superparamagnet-like properties and exhibit relaxation of their magnetization.[5] Experimentally, SMMs exhibit frequency-dependent out-of-phase alternating-current (ac) magnetic susceptibility signals and hysteresis loops, the diagnostic property of a magnet.[6] On the other hand, magnetic refrigeration is based on the magnetocaloric effect (MCE), *i.e.*, the change of magnetic entropy (ΔS_m) and adiabatic temperature (ΔT_{ad}) following a change of the applied magnetic field (ΔH), and can be used for cooling purposes *via* adiabatic demagnetization.[7]

Magnetic anisotropy, which is the directional dependence of magnetization, is a 'key' element for the design of both types of molecular magnetic materials. Highly anisotropic systems resulting from the presence of metal ions with unquenched orbital angular momenta, *i.e.*, 4f-metal ions such as Dy^{III} and Tb^{III}, may lead to prominent SMMs with large blocking temperatures and U values.[8] On the other hand, in a molecular magnetic refrigerant, it is preferable to have paramagnetic systems with negligible magnetic anisotropy (*i.e.*, Gd^{III}-containing compounds).[9] The resulting m_s or m_J states should be degenerate to increase the degrees of freedom (*i.e.*, the entropy) present at the spin ground state.[10] In addition, it is desirable for an efficient magnetic refrigerant the ground state of the system to be close in energy with the excited states, an occasion that is facilitated by the weak magnetic coupling between the metal ions present. This may lead to the enhancement of the dependence of the MCE on the applied magnetic field.[11]

To that end, a promising route to the synthesis of high-nuclearity SMMs and magnetic refrigerants is the amalgamation of paramagnetic Cu^{II} and 4f-metal ions with a suitable 'ligand blend' comprising both bridging and terminal functionalities. The bridging part of the ligands should be capable of aggregating the metal ions into a nanosized molecular structure while the terminal moieties of the ligands should prevent an extensive polymerization, which would otherwise lead to multidimensional coordination polymers. Furthermore, the magnetic coupling between Cu^{II} and lanthanides is frequently weak, albeit not negligible, and occasionally ferromagnetic,[12] thus leading to molecular species whose magnetic properties are overall dependent on the magnitude of anisotropy. To date, the Cu^{II}/Ln^{III} clusters with the record SMM and MCE values are the $\{Cu_4Dy_4\}$[13]

[a] *Department of Chemistry, Brock University, 1812 Sir Isaac Brock Way, L2S 3A1 St. Catharines, Ontario, Canada. E-mail: tstamatatos@brocku.ca; Tel: +1-905-688-5550 ext. 3400*
[b] *Department of Chemistry, University of Florida, Gainesville, Florida 32611-7200, USA*
[c] *REQUIMTE-LAQV & Department of Chemistry and Biochemistry, Faculty of Sciences, University of Porto, 4169-007 Porto, Portugal*
[d] *Department of Chemistry, Texas A&M University, College Station, Texas 77843-3255, USA*
[e] *Institut Néel, CNRS & Université Grenoble Alpes, BP 166, 25 avenue des Martyrs, 38042 Grenoble Cedex 9, France*
[f] *Physikalisches Institut, Karlsruhe Institute of Technology (KIT), Wolfgang-Gaede-Str. 1, D-76131 Karlsruhe, Germany*
[g] *Institut für Nanotechnologie, Karlsruhe Institute of Technology (KIT), Hermann-von-Helmholtz-Platz 1, D-76344 Eggenstein-Leopoldshafen, Germany*

† Electronic supplementary information (ESI) available: Complete synthetic and crystallographic discussion, structural and magnetism figures. CCDC 1531942–1531944. For ESI and crystallographic data in CIF or other electronic format see DOI: 10.1039/c7cc01382e

and $\{Cu_2Gd_7\}$[14] complexes with U_{eff} = 32.2 K (in zero external dc field) and $-\Delta S_m$ = 34.6 J kg^{-1} K^{-1} for ΔH = 9 T, respectively. We and others have had a longstanding interest in the use of pyridyl oximes and dioximes (Scheme S1, ESI†) for the synthesis of high-nuclearity molecular magnetic materials.[15] These families of organic chelating/bridging ligands are capable of binding both transition metal ions and lanthanides, thus facilitating the formation and crystallization of structurally impressive complexes.[15,16]

We herein report a new family of nanosized $\{Cu_6Ln_{12}\}$ molecular compounds with an aesthetically pleasing 'windmill'-like topology that was resulted from the combined use of bridging azides and the dianion of 2,6-diacetylpyridine dioxime ($dapdoH_2$, Scheme S1, ESI†). The $\{Cu_6Ln_{12}\}$ clusters are among the highest nuclearity Cu/Ln species reported to date[17] and, in contrast to the majority of previously reported $\{Cu_xLn_y\}$ clusters with $x \gg y$ or $x \sim y$, they exhibit a 2 : 1 Ln^{III}–to–Cu^{II} ratio.[14] Furthermore, the $\{Cu_6Dy_{12}\}$ complex shows hysteresis loops at $T < 1.1$ K and a U_{eff} of 17 K, whereas the $\{Cu_6Gd_{12}\}$ analogue exhibits a magnetic entropy change of 33.7 J kg^{-1} K^{-1} for ΔH = 7 T, among the highest values yet reported in 3d/4f-systems and the second highest in Cu/Ln chemistry after the $\{Cu_2Gd_7\}$, but for ΔH = 9 T.

The general reaction of $Cu(NO_3)_2{\cdot}3H_2O$, $Ln(NO_3)_3{\cdot}6H_2O$ (Ln = Gd^{III}, Tb^{III}, Dy^{III}), $dapdoH_2$, Me_3SiN_3, and NEt_3 in a 1 : 3 : 1 : 3 : 5 molar ratio in MeOH : H_2O (10 : 1 v/v) gave blue crystals of the octadecanuclear compounds $[Cu_6Gd_{12}(OH)_{20}(N_3)_6(NO_3)_{10}(dapdo)_6(MeOH)_{14}]{\cdot}[Cu_6Gd_{12}(OH)_{20}(N_3)_4(NO_3)_{12}(dapdo)_6(MeOH)_{10}(H_2O)_4]$ (**1**), $[Cu_6Tb_{12}(OH)_{20}(N_3)_6(NO_3)_8(dapdo)_6(H_2O)_{18}](OH)_2$ (**2**), and $[Cu_6Dy_{12}(OH)_{20}(N_3)_6(NO_3)_8(dapdo)_6(H_2O)_{18}](OH)_2$ (**3**) in good yields (>45%)(ESI†). The chemical and structural identities of the reported compounds were confirmed by single-crystal X-ray crystallography, elemental analyses (C, H, N), and IR spectral comparison (ESI†). The formulae of **1–3** are based on metric parameters, charge-balance considerations, and bond valence sum (BVS)[18] calculations on the O atoms of the OH^- groups. The presence of OH^- counterions in **2** and **3** is of precedence in high-nuclearity metal cluster chemistry.[19]

In view of the structural similarities of **1–3**, only the structure of **3** will be described as a representative example. The structures of **1** and **2** are shown in Fig. S1 and S2 (ESI†), respectively. There are two crystallographically independent $\{Cu_6Gd_{12}\}$ clusters in the crystal of **1** with similar formulae and core topologies. The molecular structure of the cation of **3** (Fig. 1, top) possesses a unique 'windmill'-like topology (Fig. 1, bottom) that results from the assembly of a central $\{Dy_6(\mu_3\text{-}OH)_8\}^{10+}$ octahedron (the 'rotor' of the 'windmill') with six external $\{CuDy_2(\mu_3\text{-}OH)\}^{7+}$ triangles (the 'blades' of the 'windmill') *via* sharing common Dy^{III} vertices (Dy1, Dy2, Dy3 and their symmetry-related partners). The linkage between the Dy^{III} atoms of the central core and the external non-planar array of alternating Cu^{II} and Dy^{III} atoms is provided by six μ-1,1 (end-on) N_3^- and six μ-bridging OH^- groups, respectively. BVS calculations on all bridging inorganic O atoms gave values in the 1.01–1.27 range confirming their assignment as OH^- groups. All doubly-deprotonated $dapdo^{2-}$ ligands bridge the external

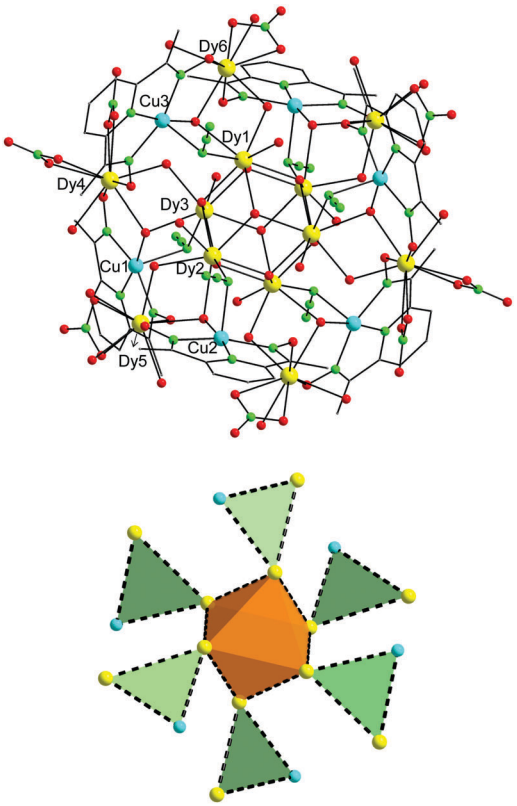

Fig. 1 Molecular structure of the cation of **3** (top) and its 'windmill'-like metal topology (bottom), consisting of a central $\{Dy_6\}$ octahedron edge-shared to six $\{CuDy_2\}$ triangles. H atoms are omitted for clarity. Color scheme: Cu^{II} cyan, Dy^{III} yellow, O red, N green, C dark gray.

Cu^{II} and Dy^{III} atoms in the same $\eta^1{:}\eta^1{:}\eta^1{:}\eta^1{:}\mu_3$ fashion, acting as tridentate N-chelates to Cu^{II} atoms and O-bridging ligands to the 4f-metal ions. The complete core of **3** is thus $\{Cu_6Dy_{12}(\mu_3\text{-}OH)_8(\mu\text{-}OH)_{12}(\mu\text{-}N_3)_6(\mu\text{-}NO)_{12}\}^{10+}$ (Fig. S3, ESI†). **1–3** are the first Cu/4f-metal complexes bearing the ligand $dapdoH_2$.

All Cu^{II} ions are five-coordinate with slightly distorted square pyramidal geometries, while Dy(1,2,3,6) and Dy(4,5), as well as their symmetry-related partners, are eight- and nine-coordinate, respectively. The coordination spheres of the 4f-metal ions were completed by eight bidentate chelating NO_3^- groups and eighteen terminal H_2O molecules. The program SHAPE[20] was used to estimate the closer coordination polyhedra defined by the donor atoms around all Dy atoms in **3**. The best fit was obtained for the square antiprismatic (Dy(1,2,3)), muffin (Dy4), spherical capped square antiprismatic (Dy5), and triangular dodecahedral (Dy6) geometries (Fig. S4, ESI†), with CShM values of 0.49, 0.48, 0.61, 1.22, 0.86, and 2.16, respectively. Values of CShM between 0.1 and 3 usually correspond to a not negligible, but still small, distortion from ideal geometry. Finally, the space-filling representation shows that **3** has a nanoscale spherical structure with dimensions of ~2 × 2 nm (Fig. S5, ESI†).

Solid-state direct-current (dc) magnetic susceptibility (χ_M) data on dried and analytically-pure samples of **1–3** were collected in the 5.0–300 K range in an applied field of 0.1 T, and are plotted as $\chi_M T$ *vs.* T in Fig. S6 (ESI†). The experimental

$\chi_M T$ values at 300 K for all complexes are in excellent agreement with the theoretical ones (96.75 cm^3 K mol^{-1} for **1**; 144.09 cm^3 K mol^{-1} for **2**; 172.29 cm^3 K mol^{-1} for **3**) for 6 Cu^{II} and 12 Ln^{III} noninteracting ions. In all complexes, the $\chi_M T$ products remain almost constant at values of ~95 (**1**), 140 (**2**), and 170 (**3**) cm^3 K mol^{-1} from 300 K to ~120 K, and then steadily decrease to minimum values of 64.55 (**1**), 97.62 (**2**), and 152.64 (**3**) cm^3 K mol^{-1} at 5.0 K, indicating the presence of predominant antiferromagnetic exchange interactions between the metal centers and/or depopulation of the excited M_J states when the 4f-metal ion is Tb^{III} or Dy^{III}. The slightly different shape of the $\chi_M T$ *vs.* T plot for the $\{Cu_6Dy_{12}\}$ complex at $T < 15$ K may be attributed to the presence of some weak intramolecular ferromagnetic exchange interactions. Because of the many different magnetic exchange pathways involved into the superexchange mechanism, it is not possible to accurately propose a ground state spin value for **1** based on a 'spin-up' *vs.* 'spin-down' vector scheme. Undoubtedly, all three complexes have fairly large spin ground states, as indicated by their large magnetic moments at 5 K, and we have therefore performed alternating-current (ac) studies for the anisotropic analogues **2** and **3** to investigate their magnetization dynamics in the absence of an external dc field.

Complex $\{Cu_6Tb_{12}\}$ did not show any out-of-phase, χ_M'', signals but the $\{Cu_6Dy_{12}\}$ analogue exhibits frequency-dependent tails of signals below ~4 K, suggestive of the magnetization relaxation of a fast-relaxing SMM (Fig. S7, ESI†). To confirm the SMM behavior of **3**, detailed magnetization (M) *vs.* dc field studies were undertaken to look for hysteresis, the diagnostic property of a magnet. The data were collected on single-crystals of **3** that had been kept in contact with mother liquor using a micro-SQUID apparatus. Hysteresis loops were indeed observed below ~1.1 K, whose coercivities increase with decreasing temperature (Fig. 2, top) and increasing field sweep rate (Fig. S8, ESI†), as expected for the superparamagnetic-like properties of an SMM below its blocking temperature. For relaxation rate *vs.* T data, the crystal's magnetization was first saturated in one direction at ~5 K with a large applied dc field, the temperature decreased to a chosen value in the 0.04–1.3 K range, and then the field was removed and the magnetization decay monitored with time (Fig. S9, ESI†). The resulting relaxation rate ($1/\tau$) *vs.* T data was then used to construct an Arrhenius-type plot, as shown in Fig. 2 (bottom). The fit to the thermally-activated region gave $\tau_0 = 3 \times 10^{-11}$ s and $U_{eff} = 17$ K. At ~0.1 K and below, the relaxation becomes temperature-independent, consistent with relaxation *via* a ground state QTM.

Magnetization (M) *vs.* field (H) studies for the $\{Cu_6Gd_{12}\}$ analogue from 2 to 10 K show a continuous increase of M as H increases, indicating the presence of weak antiferromagnetic interactions and low-lying excited states. The magnetization of **1** reaches a maximum value of 88.8 $N\mu_B$ at 7 T, very close to the maximum value of 90 $N\mu_B$ expected for 6 Cu^{II} and 12 Gd^{III} coupled ions (Fig. S10, ESI†). The large value of the magnetization renders **1** a possible candidate for low-temperature magnetic cooling, and we have thus evaluated its MCE by calculating the magnetic entropy change, ΔS_m, for selected applied field changes using the magnetization data and the Maxwell

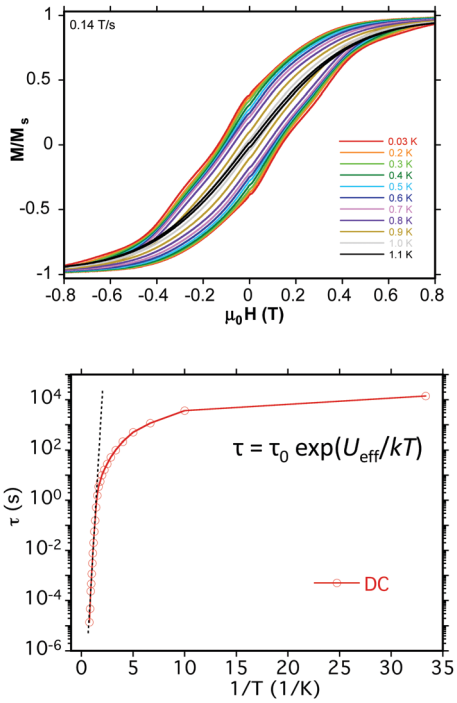

Fig. 2 (top) Magnetization (M) *vs.* applied dc field ($\mu_0 H$) hysteresis loops for a single-crystal of **3** at the indicated temperatures, and (bottom) Arrhenius-type plot of the relaxation time (τ) *vs.* $1/T$ of **3** using data obtained from the dc magnetization decay measurements at the low temperature regime. The dashed line is the fit of data in the thermally-activated region to the Arrhenius equation; see the text for the fit parameters. The magnetization is normalized to its saturation value (M_s).

equation: $\Delta S_m(T, \Delta H) = \int_{H_i}^{H_f} \left[\frac{\partial M(T,H)}{\partial T}\right]_H dH$ (Fig. 3). We report an appreciable value of $-\Delta S_m$ which reaches ~33.7 J kg^{-1} K^{-1} at $T = 3$ K for $\Delta H = 7$ T. This is what we could expect considering the large net magnetic moment and negligible anisotropy of the molecule, as well as the weak intra-cluster interactions involving Gd^{III} ions that lead to low-lying excited spin states. However, this value is still lower than the maximum entropy value per mole ($29.11R$ ~47.4 J kg^{-1} K^{-1})[21] for 6 Cu^{II} and 12 Gd^{III} fully decoupled ions, suggesting that larger fields are necessary to

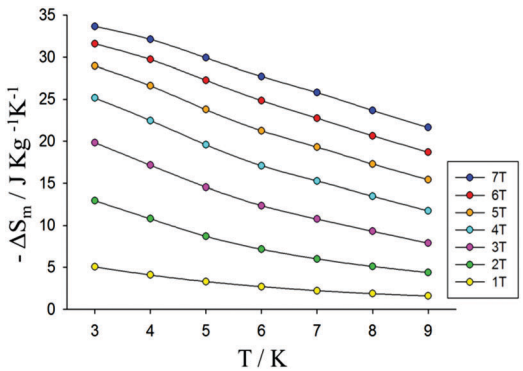

Fig. 3 Magnetic entropy changes of **1**, as obtained from magnetization data at various fields and temperatures.

overcome completely the strength of the interactions and decouple the Cu^{II} and Gd^{III} spins.

In conclusion, we have shown that the self-assembly reaction of $Cu(NO_3)_2{\cdot}3H_2O$ with various lanthanides in the presence of the pentadentate organic chelate, 2,6-diacetylpyridine dioxime, and azides has led to a unique family of 'windmill'-like $\{Cu_6Ln_{12}\}$ clusters with diverse magnetic properties depending on the 4f-metal ion present. The $\{Cu_6Dy_{12}\}$ analogue was confirmed to be a SMM with an energy barrier for the magnetization reversal of 17 K, one of the highest U_{eff} values reported to date for Cu^{II}/Ln^{III} SMMs. Furthermore, the $\{Cu_6Gd_{12}\}$ complex was shown to exhibit a large magnetic entropy change of $\sim$33.7 J kg^{-1} K^{-1} at T = 3 K, rendering it a promising molecular magnetic refrigerant for low-temperature cooling applications. Work in progress includes the synthesis and magnetic characterization of additional members of this family of $\{Cu_6Ln_{12}\}$ complexes, as well as the deliberate replacement of Cu^{II} by other divalent 3d-metal ions, as a means of altering the structural and/or physical properties of the resulting molecular materials.

This work was supported by NSERC-DG (Th. C. S), ERA (Th. C. S), Brock University (Chancellor's Chair for Research Excellence; Th. C. S), and NSF grant CHE-1565664 (to G. C). L. C.-S. acknowledges financial support from FCT/MCTES (Fundação para a Ciência e a Tecnologia/Ministério da Ciência, Tecnologia e Ensino Superior, Portugal) with national funds and was also co-financed by FEDER (Fundo Europeu de Desenvolvimento Regional, European Union) under the partnership agreement PT2020, through the research centre REQUIMTE-LAQV (UID/QUI/50006/2013 – POCI/01/0145/FEDER/007265). W. W acknowledges the Alexander von Humboldt foundation. K. M. P. would like to thank the NHMFL for partial funding. The NHMFL is supported by NSF/DMR grant DMR-1157490 and the State of Florida.

Notes and references

1 C. Papatriantafyllopoulou, E. E. Moushi, G. Christou and A. J. Tasiopoulos, *Chem. Soc. Rev.*, 2016, **45**, 1597.
2 (*a*) A. J. Tasiopoulos, A. Vinslava, W. Wernsdorfer, K. A. Abboud and G. Christou, *Angew. Chem., Int. Ed.*, 2004, **43**, 2117; (*b*) G. F. S. Whitehead, F. Moro, G. A. Timco, W. Wernsdorfer, S. J. Teat and R. E. P. Winpenny, *Angew. Chem., Int. Ed.*, 2013, **125**, 10116; (*c*) M. Manoli, R. Inglis, M. J. Manos, V. Nastopoulos, W. Wernsdorfer, E. K. Brechin and A. J. Tasiopoulos, *Angew. Chem., Int. Ed.*, 2011, **50**, 4441; (*d*) P. Alborés and E. Rentschler, *Angew. Chem., Int. Ed.*, 2009, **48**, 9366.
3 (*a*) C. J. Milios and R. E. P. Winpenny, *Struct. Bonding*, 2015, **164**, 1; (*b*) R. Sessoli and A. K. Powell, *Coord. Chem. Rev.*, 2009, **253**, 2328; (*c*) H. L. Feltham and S. Brooker, *Coord. Chem. Rev.*, 2014, **276**, 1.
4 M. Evangelisti, Molecule-Based Magnetic Coolers: Measurement, Design and Application, in *Molecular Magnets: Physics and Applications*, J. Bartolomé, F. Luis, J. F. Fernández, ed. 2014, Springer, Verlag Berlin Heidelberg, pp. 365–387.
5 D. Gatteschi, R. Sessoli and J. Villain, *Molecular Nanomagnets*, 2006, Oxford University Press, Oxford.
6 R. Bagai and G. Christou, *Chem. Soc. Rev.*, 2009, **38**, 1011.
7 (*a*) M. Evangelisti, F. Luis, L. J. de Jongh and M. Affronte, *J. Mater. Chem.*, 2006, **16**, 2534; (*b*) M. Evangelisti and E. K. Brechin, *Dalton Trans.*, 2010, **39**, 4672.
8 (*a*) D. N. Woodruff, R. E. P. Winpenny and R. A. Layfield, *Chem. Rev.*, 2013, **113**, 5110; (*b*) J. D. Rinehart and J. R. Long, *Chem. Sci.*, 2011, **2**, 2078.
9 J. W. Sharples, D. Collison, E. J. L. McInnes, J. Schnack, E. Palacios and M. Evangelisti, *Nat. Commun.*, 2014, **5**, 5321.
10 J. W. Sharples and D. Collison, *Polyhedron*, 2013, **54**, 91.
11 (*a*) J. W. Sharples, Y.-Z. Zheng, F. Tuna, E. J. L. McInnes and D. Collison, *Chem. Commun.*, 2011, **47**, 7650; (*b*) M. Evangelisti, O. Roubeau, E. Palacios, A. Camón, T. N. Hooper, E. K. Brechin and J. J. Alonso, *Angew. Chem., Int. Ed.*, 2011, **50**, 6606.
12 For example, see: (*a*) S. Langley, N. F. Chilton, B. Moubaraki, T. Hooper, E. K. Brechin, M. Evangelisti and K. S. Murray, *Chem. Sci.*, 2011, **2**, 1166; (*b*) T. N. Hooper, J. Schnack, S. Piligkos, M. Evangelisti and E. K. Brechin, *Angew. Chem., Int. Ed.*, 2012, **51**, 4633; (*c*) O. Kahn, *Molecular Magnetism*, VCH Publishers, New York, 1993; (*d*) M. Andruh, I. Ramade, E. Codjovi, O. Guillou, O. Kahn and J.-C. Trombe, *J. Am. Chem. Soc.*, 1993, **115**, 1822.
13 J. Wu, L. Zhao, M. Guoab and J. Tang, *Chem. Commun.*, 2015, **51**, 17317.
14 S. K. Langley, B. Moubaraki, C. Tomasi, M. Evangelisti, E. K. Brechin and K. S. Murray, *Inorg. Chem.*, 2014, **53**, 13154.
15 (*a*) C. J. Milios, Th. C. Stamatatos and S. P. Perlepes, *Polyhedron*, 2006, **25**, 134; (*b*) D. I. Alexandropoulos, C. Papatriantafyllopoulou, C. Li, L. Cunha-Silva, M. J. Manos, A. J. Tasiopoulos, W. Wernsdorfer, G. Christou and Th. C. Stamatatos, *Eur. J. Inorg. Chem.*, 2013, 2286; (*c*) A. Escuer, J. Esteban, N. Aliaga-Alcalde, M. Font-Bardia, T. Calvet, O. Roubeau and S. J. Teat, *Inorg. Chem.*, 2010, **49**, 2259.
16 (*a*) C. Papatriantafyllopoulou, Th. C. Stamatatos, C. G. Efthymiou, L. Cunha-Silva, F. A. Almeida Paz, S. P. Perlepes and G. Christou, *Inorg. Chem.*, 2010, **49**, 9743; (*b*) C. D. Polyzou, H. Nikolaou, C. Papatriantafyllopoulou, V. Psycharis, A. Terzis, C. P. Raptopoulou, A. Escuer and S. P. Perlepes, *Dalton Trans.*, 2012, **41**, 13755.
17 For high-nuclearity Cu^{II}/Ln^{III} clusters, see: (*a*) J.-D. Leng, J.-L. Liu and M.-L. Tong, *Chem. Commun.*, 2012, **48**, 5286; (*b*) D. Dermitzaki, G. Lorusso, C. P. Raptopoulou, V. Psycharis, A. Escuer, M. Evangelisti, S. P. Perlepes and Th. C. Stamatatos, *Inorg. Chem.*, 2013, **52**, 10235; (*c*) G. Xiong, H. Xu, J. Z. Cui, Q. L. Wang and B. Zhao, *Dalton Trans.*, 2014, **43**, 5639; (*d*) S. Xiang, S. Hu, T. Sheng, R. Fu, X. Wu and X. A. Zhang, *J. Am. Chem. Soc.*, 2007, **129**, 15144; (*e*) L. Zhang, L. Zhao, P. Zhang, C. Wang, S.-W. Yuan and J. Tang, *Inorg. Chem.*, 2015, **54**, 11535; (*f*) J. Wu, L. Zhao, L. Zhang, X.-L. Li, M. Guo, A. K. Powell and J. Tang, *Angew. Chem., Int. Ed.*, 2016, **55**, 15574; (*g*) J. Wu, L. Zhao, L. Zhang, X.-L. Li, M. Guo and J. Tang, *Inorg. Chem.*, 2016, **55**, 5514.
18 I. D. Brown and D. Altermatt, *Acta Crystallogr., Sect. B: Struct. Sci.*, 1985, 244. An O BVS in the $\sim$1.7–2.0, $\sim$1.0–1.2, and $\sim$0.2–0.4 ranges is indicative of non-, single- and double-protonation, respectively.
19 For example, see: (*a*) E. Moushi, C. Lampropoulos, W. Wernsdorfer, V. Nastopoulos, G. Christou and A. J. Tasiopoulos, *J. Am. Chem. Soc.*, 2010, **132**, 16146; (*b*) Th. C. Stamatatos, V. Nastopoulos, A. J. Tasiopoulos, E. Moushi, W. Wernsdorfer, G. Christou and S. P. Perlepes, *Inorg. Chem.*, 2008, **47**, 10081.
20 S. Alvarez, P. Alemany, D. Casanova, J. Cirera, M. Llunell and D. Avnir, *Coord. Chem. Rev.*, 2005, **249**, 1693.
21 The molecular mass used for the calculation of the ΔS_m of **1** in units of J kg^{-1} K^{-1} was 5104.3 g mol^{-1}, which is the average value accounted for the presence of both crystallographically independent $\{Cu_6Gd_{12}\}$ clusters in the crystal of **1**.